Daily Cropland Soil NO_x Emissions Identified by TROPOMI and SMAP

Daniel E. Huber[1], Allison L. Steiner[1], Eric A. Kort[1]

[1]Department of Climate and Space Sciences and Engineering, University of Michigan, Ann Arbor, MI, USA

Corresponding author: Daniel Huber (dehuber@umich.edu)

Key Points:

- Daily TROPOMI data provide new opportunities to observe regional cropland NO_x emissions from space
- Soil NO_x pulsing is identified throughout the growing season with a NO_x maximum observed when soils dry to ~30% volumetric soil moisture
- Cropland NO_x emissions peak at the onset of the growing season as determined by TROPOMI NO_2 enhancements and a box model framework

This is the author manuscript accepted for publication and has undergone full peer review but has not been through the copyediting, typesetting, pagination and proofreading process, which may lead to differences between this version and the Version of Record. Please cite this article as doi: 10.1029/2020GL089949

Abstract

We use TROPOMI (TROPOspheric Monitoring Instrument) tropospheric nitrogen dioxide (NO_2) measurements to identify cropland soil nitrogen oxide ($NO_x = NO + NO_2$) emissions at daily to seasonal scales in the United States Southern Mississippi River Valley. Evaluating 1.5 years of TROPOMI observations with a box model, we observe seasonality in local NO_x enhancements and estimate maximum cropland soil NO_x emissions (15-34 ng N m^{-2} s^{-1}) early in growing season (May-June). We observe soil NO_x pulsing in response to daily decreases in volumetric soil moisture (VSM) as measured by the Soil Moisture Active Passive (SMAP) satellite. Daily NO_2 enhancements reach up to 0.8 x 10^{15} molecules cm^{-2} 4-8 days after precipitation when VSM decreases to ~30%, reflecting a VSM that is wetter than previously defined NO_x pulse events. This demonstrates that TROPOMI NO_2 observations, combined with observations of underlying process controls (e.g. soil moisture), can constrain soil NO_x processes from space.

Plain Language Summary

Soils are a known source of atmospheric nitrogen oxides ($NO_x = NO + NO_2$), a pollutant that contributes to poor air quality. In cropland regions, where nitrogen-rich fertilizers are applied to soils, NO_x emissions can be significantly enhanced. We use satellite observations of nitrogen dioxide (NO_2) from TROPOMI (TROPOspheric Monitoring Instrument) to quantify the soil-driven contribution to the amount of NO_x in the atmosphere in a cropland region in Mississippi, United States. At the daily level, we use TROPOMI measurements together with soil moisture observations from the SMAP (Soil Moisture Active Passive) satellite to show that soil moisture plays an important role in regulating the amount of NO_x that cropland soils release. At the seasonal level, we see the largest NO_x contribution from soils toward the beginning of the growing season (May-June).

1. Introduction

Soils are a significant source of nitrogen oxides ($NO_x = NO + NO_2$) to the atmosphere, contributing up to 40% of the nitrogen dioxide (NO_2) column over cropland during northern hemisphere summer months (Hudman et al., 2012; Vinken et al., 2014). Fossil NO_x emissions, the largest source of NO_x in the troposphere, decreased on average by 5.9% yr^{-1} from 2005-2017, increasing the relative contribution from soil NO_x to overall NO_x emissions (Jiang et al., 2018;

Silvern et al., 2019). NO_x is a primary air pollutant associated with the formation of secondary pollutants including ozone (O_3) and nitrogen-based aerosols (Jenkin & Clemitshaw, 2000). NO_x and its subsequent oxidation products are not only detrimental to human health, but they can also cause adverse impacts for plants and other living organisms (Ashmore, 2005; Kampa & Castanas, 2008). As soil NO_x continues to represent a larger portion of total global NO_x, it will be increasingly important to understand its emission on finer temporal and spatial scales.

Soil NO_x is primarily emitted in the form of nitric oxide (NO) with emissions driven by microbial processes within the soil surface layer (Pilegaard, 2013). The activity of NO-producing bacteria is determined by environmental conditions such as water-filled pore space (WFPS), soil temperature and defining soil characteristics such as texture, bulk density and nitrogen availability (Ludwig et al., 2001). WFPS plays a key role in controlling the magnitude of soil NO_x emissions, as the activity of bacteria that drive emissions is highly dependent on the ratio of water to oxygen in the soil pore space. The relative magnitude of soil NO_x emissions as a function of WFPS is typically represented by a Poisson function, with weakest emissions at extreme lower and upper limits of WFPS, and strongest relative emissions between 20% and 65% WFPS (Hudman et al., 2012; Pilegaard et al., 2013), dependent upon specific soil characteristics. Increased nitrogen availability in cropland soils, largely due to fertilizer application, greatly enhances soil NO_x emissions (Oikawa et al., 2015; Bouwman et al., 2002), making croplands important sources contributing to the regional NO_x budget.

Current process understanding of soil NO_x emissions has been driven by small-scale (~1m) chamber studies, with emissions identified from a variety of soil and ecosystem types (e.g. Levine et al., 1996; Eberwein et al., 2020; Schindlbacher et al., 2004; Roelle et al. 2001). These and other observational studies of soil NOx fluxes have been used to develop process-based emissions models to estimate soil NO_x emissions, such as the Berkeley Dalhousie Soil NO_x Parameterization (BDSNP) (Hudman et al., 2012). BDSNP has been implemented into chemical transport models, including the GEOS-Chem global model and CMAQ regional model (Hudman et al., 2012; Rasool et al, 2016). BDSNP represents the effects of environmental variables on the magnitude of emissions, including WFPS, soil temperature, soil nitrogen availability, soil biome and the contribution to emissions from soil NO_x pulsing. NO_x pulsing refers to enhanced emissions that can occur after the first soil wetting following an extended dry period. The wetting of dry soil can

reinvigorate previously dormant soil bacteria, resulting in NO emissions pulses that can be many times the pre-pulse emissions magnitude (Kim et al., 2012). The pulsing mechanism within the BDSNP is based on Yan et al. (2005), which activates once soils dry to a volumetric soil moisture (VSM) of 17.5% or less for at least three consecutive days prior to soil wetting.

Space-based observations are particularly useful for understanding soil NO_x emissions in regions where ground-based observations are not available. Using SCIAMACHY (Scanning Imaging Absorption spectroMeter for Atmospheric CHartographY) and a soil NO_x emissions model, Bertram et al. (2005) identified daily soil NOx pulse emissions of up to 25 ng N m^{-2} s^{-1} in an agricultural region in Montana, with peak emissions at the beginning of the growing season. A global study used observed NO_2 vertical column densities (VCDs) from the Ozone Monitoring Instrument (OMI) and the GEOS-Chem model to quantify average June northern hemisphere soil NO_x emissions at 2.5° resolution (Vinken et al., 2014). Multiple satellite studies have observed soil NO_x emissions and pulsing in the African Sahel (Jaeglé et al., 2004; Zörner et al., 2016; Hickman et al., 2018), where NO_2 column enhancements up to 100% of the pre-pulse VCDs are attributed to soil NO_x pulsing associated with the onset of the rainy season following months of dry weather (Zörner et al., 2016).

While satellite observations have been used to identify soil NO_x emissions in the past, no satellite study has yet constrained emissions at near-daily regional scales and in conjunction with satellite-observed process controls. In this study, we utilize satellite observations of tropospheric NO_2 from TROPOMI (TROPOspheric Monitoring Instrument) to quantify the contribution of cropland soils to regional NO_x emissions in the lower Mississippi (MS) River Valley on daily to seasonal scales in 2018 and 2019. The unprecedented resolution of the TROPOMI product allows for soil emission processes to be evaluated using observed NO_2 enhancements at spatiotemporal scales unresolvable with previous space-based NO_2 products. We identify a robust seasonally varying contribution from cropland soils to NOx emissions, with the largest contributions during the late spring months (May-June), with emissions patterns matching predictions by the BDSNP model. Further, we use daily TROPOMI tropospheric NO_2 observations in conjunction with Soil Moisture Active Passive (SMAP) VSM observations to identify NO_x pulse events in the days following precipitation, a consistently observed feature for this domain distinct from the historical definition of soil NO_x pulsing.

2. Data

Level 2 tropospheric NO_2 VCD measurements are obtained from the TROPOMI instrument onboard the Sentinel-5P satellite (Veefkind et al., 2012). TROPOMI was launched in 2017, and measures NO_2 VCDs with a nadir spatial resolution of 3.5 x 7 km^2 for observations between 30 April 2018 and 06 August 2019, and a resolution of 3.5 x 5.5 km^2 from 06 August 2019 onward. TROPOMI uses observed radiation in the near-UV and visible together with a chemical transport model to estimate tropospheric NO_2 VCDs. We filter the TROPOMI data using only pixels with "flag_value" greater than or equal to 0.75 (Van Geffen et al., 2019) to remove pixels that have unreliable measurements (e.g. due to the presence of clouds). To ensure that a sufficient number of pixels remain within the region of interest after applying this filter, we require (1) a threshold of 30 pixels must remain within the domain after filtering based on the flag value alone, and (2) the number of filtered pixels divided by the total number of pixels before filtering must be greater than or equal to 25%. If at least one of these conditions is not met, then the daily swath is excluded from analysis.

Level 3 surface VSM observations are obtained from the SMAP satellite (Entekhabi et al., 2010). SMAP was launched in 2015 and uses a passive microwave radiometer to observe surface radiation in the L-band (1.4 GHz) to determine VSM mixing ratios in approximately the top 5 cm of soil. Measuring radiation at these wavelengths allows observations to be made in even very cloudy conditions, resulting in more temporally homogenous observations than TROPOMI NO_2 observations, which are impacted by the presence of clouds. To ensure that SMAP VSM is measured from soils and not overlying vegetation, we apply a filter to remove pixels with vegetation water content greater than 5 kg m^{-2} (Colliander et al., 2017).

Daily winds are derived from ERA5 reanalysis (Hersbach et al., 2020) for 18:00 - 19:00 UTC, coincident with the TROPOMI overpass. Daily precipitation totals are from the NOAA CPC Gauge-Based precipitation analysis (Chen et al., 2008). For the quantification of soil NO_x emissions, anthropogenic NO_x emissions are obtained from the 2014 gridded National Emissions Inventory (NEI) (Strum et al., 2017).

3. NO_2 and Cropland in the Mississippi River Valley

We define a 0.75 x 0.75 degree cropland domain located in the southern U.S. within the MS Delta (Fig. 1a, solid white box). Soybean is the dominant crop type, representing nearly 80% of the cropland area as determined by the CropScape database (Han et al., 2012). This region experiences year-round precipitation, with 28% and 19% of the annual precipitation occurring during the spring (MAM) and summer (JJA) seasons, respectively. This region regularly experiences changes in soil moisture due to rainfall as well as seasonal flooding from the MS River, which makes this an ideal location for studying the impact of soil moisture changes on soil NO_x emissions. Multiple powerplants are located north of the study region that can substantially contribute to the local NO_x signature. Limiting our analysis to the MS Delta, which is located more than 125 km from the nearest major urban region or major powerplants, greatly minimizes the influence of fossil NO_x emissions on the cropland NO_x signature. The cropland region has an east-west extent of approximately 70 km and is adjacent to forest on both the eastern and western edges of the region.

Individual TROPOMI overpasses can spatially resolve increased NO_2 VCDs over the cropland domain during drydown periods in days following precipitation (Fig. 1). NO_2 VCDs are relatively

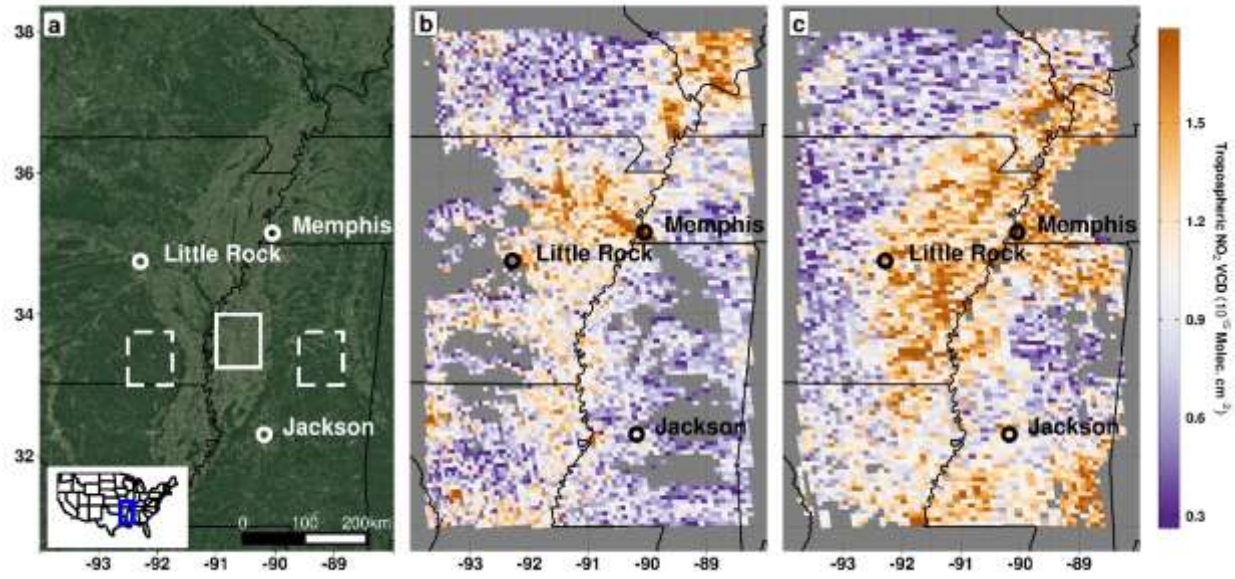

Figure 1:(a) Satellite image of the Mississippi Delta study region showing cropland (solid white box) and upwind (dashed white boxes) domains used to calculate daily NO_2 enhancements. Light green regions are primarily cropland, dark green regions are primarily forest. (b) TROPOMI tropospheric NO_2 VCDs on May 14, 2019, five days before a precipitation event. (c) TROPOMI tropospheric NO_2 VCDs on May 24, 2019, five days after a precipitation event, with enhanced NO_2 VCDs over cropland indicative of a drydown soil NO_x emissions pulse.

low over the cropland region five days before a rainfall event (Fig. 1b; 14 May 2019) yet increase five days after (Fig. 1c; 24 May 2019). Common features in the NO_2 signal are evident on both days, including the anthropogenic NO_x signature from fuel combustion sources near Little Rock, AR and Memphis, TN. However, the higher NO_2 VCDs present over the cropland after the rainfall event (Fig. 1c) suggest crop-driven soil NO_x emissions in this region.

4. Results

4.1 NO_2 Column Enhancement

We use forested regions upwind of the cropland domain as reference sites to estimate daily average background TROPOMI NO_2 VCDs (Fig. 1a, dashed white boxes). These reference sites provide nearby, "clean" upwind domains containing few major NO_x sources, which are ideal for background quantification. The reference sites facilitate the calculation of the NO_2 column enhancement over the cropland domain by subtracting the average inflow background NO_2 VCD from the average cropland NO_2 VCD. This calculated difference reveals the contribution from cropland soils to the NO_2 column for each day of available TROPOMI observations. A positive enhancement indicates higher cropland NO_2 VCDs for that day, and a negative enhancement indicates higher upwind NO_2 VCDs for that day. Upwind domains have been used in previous satellite studies to estimate background concentrations of atmospheric trace gases to derive enhancements (e.g. Kort et al., 2012) and offer a slight improvement over defining enhancements when using the lowest decile of observations (e.g. De Gouw et al., 2020). The high density of TROPOMI observations enables statistically robust daily evaluation of enhancements even considering the 30-pixel requirement (see Section 2) for both the upwind and cropland domains.

Depending upon the predominant wind direction, one of two different 0.75 x 0.75 degree upwind domains are defined for calculating the daily NO_2 enhancement: one east and one west relative to the cropland domain (Fig. 1a and Fig. S1). Days with a predominantly northly wind (340° – 20°) are excluded due to the potential influence of urban emissions from the Memphis metropolitan region. Over the analysis period (2018-2019), the east domain is used for 37% of the daily enhancements, the west domain is utilized for 50% of the daily enhancements, and about 13% of days are excluded due to the presence of a predominantly northly wind.

4.2 Seasonal NO_2 Enhancements and Soil NO_x Emissions Estimate

Monthly averaged NO_2 enhancements are largest in May 2018 and June 2019 (Fig. 2a), months that coincide with the onset of the growing season and an increase in agricultural activity. The average monthly enhancements during these months are between 0.4 - 0.5 x 10^{15} molecules cm^{-2}. Enhancements in winter months are mostly negligible, coinciding with a relative lack of agricultural activity and resulting in similar NO_2 VCDs over the cropland and upwind domains. Additionally, the timing of crop planting in the region largely shifts from May in 2018 to June in 2019 (reported by USDA NASS, Fig. S2), suggesting that the shift in the largest TROPOMI enhancements from May in 2018 to June in 2019 is a direct result of the delayed planting of crops within the cropland domain. The magnitudes of these peak monthly enhancements are consistent with Vinken et al. (2014) that estimated an absolute contribution from soils to the NO_2 column over cropland in the midwestern U.S. of approximately 0.6 x 10^{15} molecules cm^{-2} using the OMI satellite. However, Vinken et al. (2014) did not identify a contribution from soils to the NO_2 column over the MS Delta cropland domain used within this study. This may be due to the coarser resolution of the model used (2.5°), coarser resolution of OMI relative to TROPOMI or the higher fossil NO_x emissions during the study period (2005) that potentially masked the soil NO_x signal.

To estimate soil NO_x emissions (E_{soil}: ng N m^{-2} s^{-1}) from the cropland domain using TROPOMI NO_2 observations, we apply a box model that accounts for sources and sinks of NO_x:

$$E_{soil} = \frac{U\,\Delta(NO_{2,VCD})}{L} + \frac{V_d\,NO_{2,VCD}}{Z_{PBL}} + \frac{NO_{2,VCD}}{\tau} - E_{NEI} \qquad Eq.\ 1$$

where the first term on the right-hand side ($\frac{U\,\Delta(NO_{2,VCD})}{L}$) represents the advection of NO_x into the box, U is the average wind speed (m s^{-1}) over the cropland domain, $\Delta(NO_{2,VCD})$ is the spatial TROPOMI NO_2 column enhancement (molec. m^{-2}) between the cropland and upwind domain, and L is the distance (m) from edge to edge between the cropland and the upwind domain (Fig. 1a). The second term on the right-hand side represents the deposition of NO_x, where V_d is the NO_2 deposition velocity (m s^{-1}) from Yang et al. (2010), $NO_{2,VCD}$ is the NO_2 VCD (molec. m^{-2}) over the cropland domain, and Z_{PBL} is the boundary layer height estimated at a constant 10^3 m height throughout the year. The third term on the right-hand side represents the NO_x chemical loss rate, where $\frac{1}{\tau}$ is the inverse NO_x lifetime (s^{-1}). The NO_x lifetime τ is estimated to vary sinusoidally throughout a year, with a peak lifetime on December 21 and a minimum lifetime on June 21. E_{NEI}

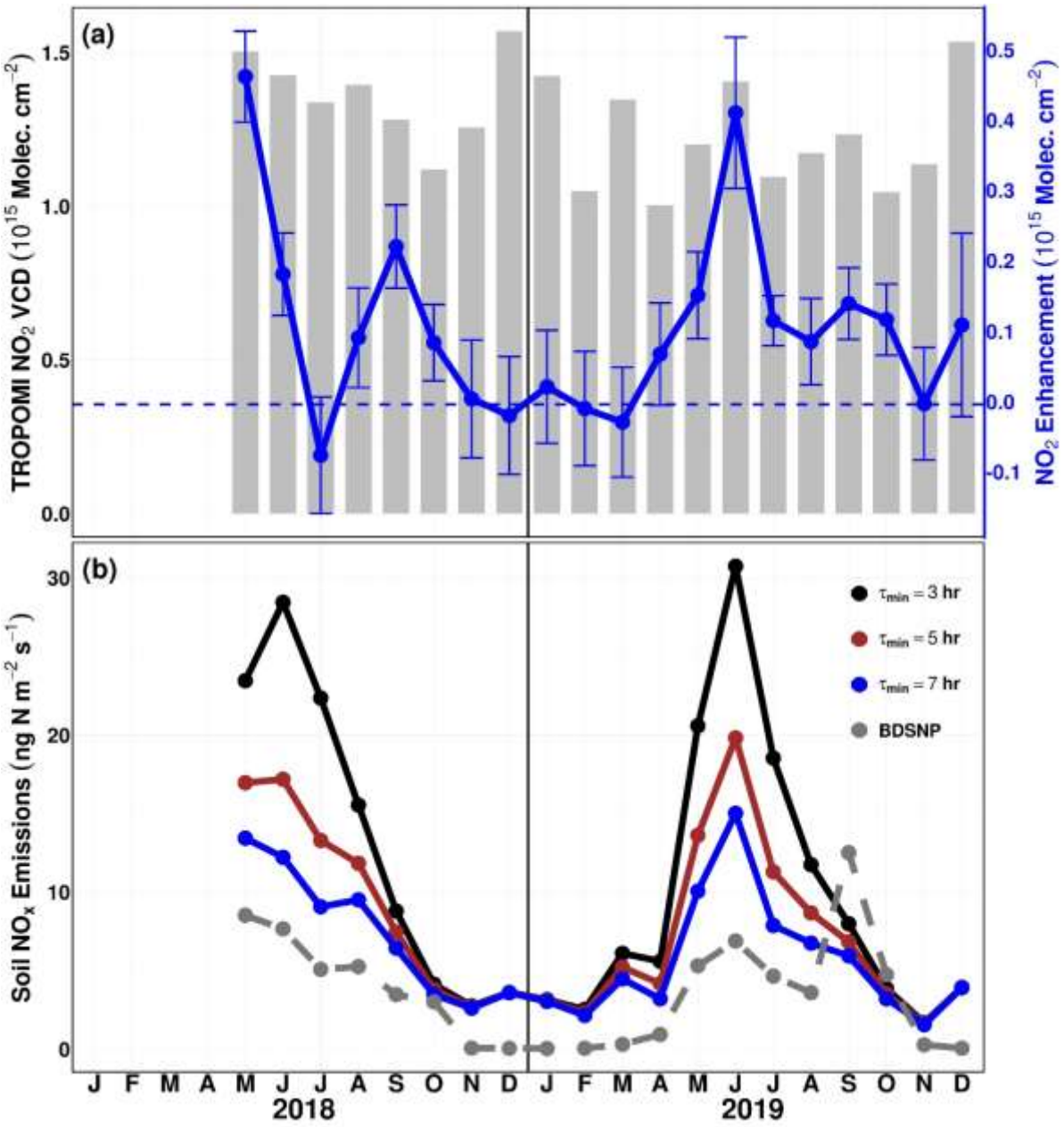

Figure 2: (a) Mean monthly TROPOMI tropospheric NO_2 VCD (gray bars; left axis) and mean monthly NO_2 column enhancement (blue line; right axis). NO_2 enhancements represent the mean monthly contribution from cropland soils to the NO_2 column. Error bars show standard error of the mean. (b) Monthly average soil NO_x emissions estimated using the soil NO_x emissions box model and the BDSNP model. All three box model scenarios converge to a December NO_x lifetime of 15 hours.

is the anthropogenic NO_x emissions (molec. m^{-2} s^{-1}) from the 2014 NEI inventory. Chemical production as a source of NO_x is assumed to be negligible.

Using equation 1, we calculate daily box model estimates of soil NO_x emissions and average to monthly values (Fig. 2b). We present three different emissions scenarios with a varying minimum June NO_x lifetime of 3, 5 and 7 hours. Martin et al. (2003) estimated NO_x lifetime of approximately 5 hours in the summer at this latitude, and we increase and decrease the summer lifetime by ± 2 hours to illustrate the sensitivity of the box model emissions estimates to NO_x lifetime assumptions. All three scenarios converge to a maximum December NO_x lifetime of 15 hours. The largest emissions occur during the late spring and early summer, with minimal emissions during the winter. Our monthly average box model emissions estimates range from 15 to 34 ng N m^{-2} s^{-1} in May and June, with the range driven by the influence of NO_x lifetime as described in recent studies (e.g. Laughner et al., 2019; Shah et al., 2020).

For the same domain and time frame, we estimate emissions using the BDSNP model. As inputs for the BDSNP, we use WFPS calculated from SMAP surface VSM observations, ERA5 soil temperature (Hersbach et al., 2020) and soil nitrogen availability data available from the MEGAN biogenic emissions model framework (Guenther et al., 2006). WFPS is calculated from the ratio of SMAP VSM to estimated soil porosity within the cropland domain (Linn and Doran, 1984). BDSNP soil NO_x emission magnitudes are roughly half that of the box model emissions with a 5-hour June lifetime, however the month-to-month variability between the two methods is consistent (Fig. 2b). Both methods estimate relative peak emissions in May of 2018 and June of 2019. Further, both methods experience similar month-to-month variability during the growing season. The exception to this is September of 2019, during which BDSNP estimates the largest monthly average emissions for the entire study period.

Our satellite-based soil NO_x emission estimates are largely consistent with small-scale chamber studies as well as satellite studies. A chamber study over cropland in North Carolina, U.S. measured average NO Emissions on the order of 20.2 ± 19 ng N m^{-2} s^{-1} during spring and summer (Roelle et al., 2001), while a chamber study in high-temperature croplands in Southern California observed median emissions of 20 ng N m^{-2} s^{-1} with individual measurements up to 900 ng N m^{-2} s^{-1} (Oikawa et al., 2015). Satellite studies show similar ranges, with Bertram et al. (2005) using SCIAMACHY to estimate May soil NO_x emissions from cropland in Montana, U.S. with daily values ranging from 10 to 25 ng N m^{-2} s^{-1} and Jaeglé et al. (2004) used the Global Ozone

Monitoring Experiment (GOME) instrument to estimate average June soil NO_x emissions from the Sahel region of 20 ng N m^{-2} s^{-1} under the assumption of a 7-hour NO_x lifetime.

4.3 Daily-scale NO_2 Enhancements and Multi-day NO_x Pulse Events

To observe the relationship between soil emissions and soil moisture within the cropland domain, we use SMAP VSM observations to identify soil drydown events that occur in the days following precipitation and observe changes in daily TROPOMI NO_2 enhancements during those events. We identify days in 2018 and 2019 between May and October with heavy (≥ 1 cm) precipitation followed by at least one week without heavy precipitation. We require observed VSM to increase to greater than 0.4 cm^3 cm^{-3} in response to the initial precipitation, and then decrease in the week following without a subsequent increase. If a relative peak in TROPOMI NO_2 enhancements occurs as SMAP observations decrease in the week following precipitation, then the peak enhancement is associated with a "drydown NO_x pulse" event.

Using the above criteria, we identify nine potential drydown NO_x pulse events between May and October in 2018 and 2019. Two drydown events are excluded due to the absence of TROPOMI data. One event is excluded due to persistently high TROPOMI enhancements occurring before, during and after soil drying. We align the remaining six events onto the same day axis, defining day 0 as the day of relative peak NO_2 enhancement following the decrease in soil moisture (Fig. 3). NO_2 enhancements increase as the soil dries and enhancements reach a relative maximum on day 0, coincident with VSM decreasing below a value of 0.3 cm^3 cm^{-3}. This suggests a local SMAP VSM threshold of approximately 30%, an emergent observation below which soils must decrease for drydown pulse emissions to reach a maximum. A previous study has shown that SMAP observations may exhibit faster soil drying than in situ measurements (Shellito et al., 2016), which would suggest that the observed threshold may be offset from in-situ measured soil moisture. Notably, in a chamber study on cropland NO emissions in California, Oikawa et al. (2015) found peak soil NO_x emissions occurred at roughly 30% VSM, suggesting this 30% threshold may hold broader significance for cropland soils. We evaluate the significance of each day 0 NO_2 column enhancement by conducting two-sample t-tests between upwind and cropland domain observations for all six events, confirming the significance of the observed enhancements (p-values < 0.05 for five of six events, p-value $= 0.09$ for remaining event).

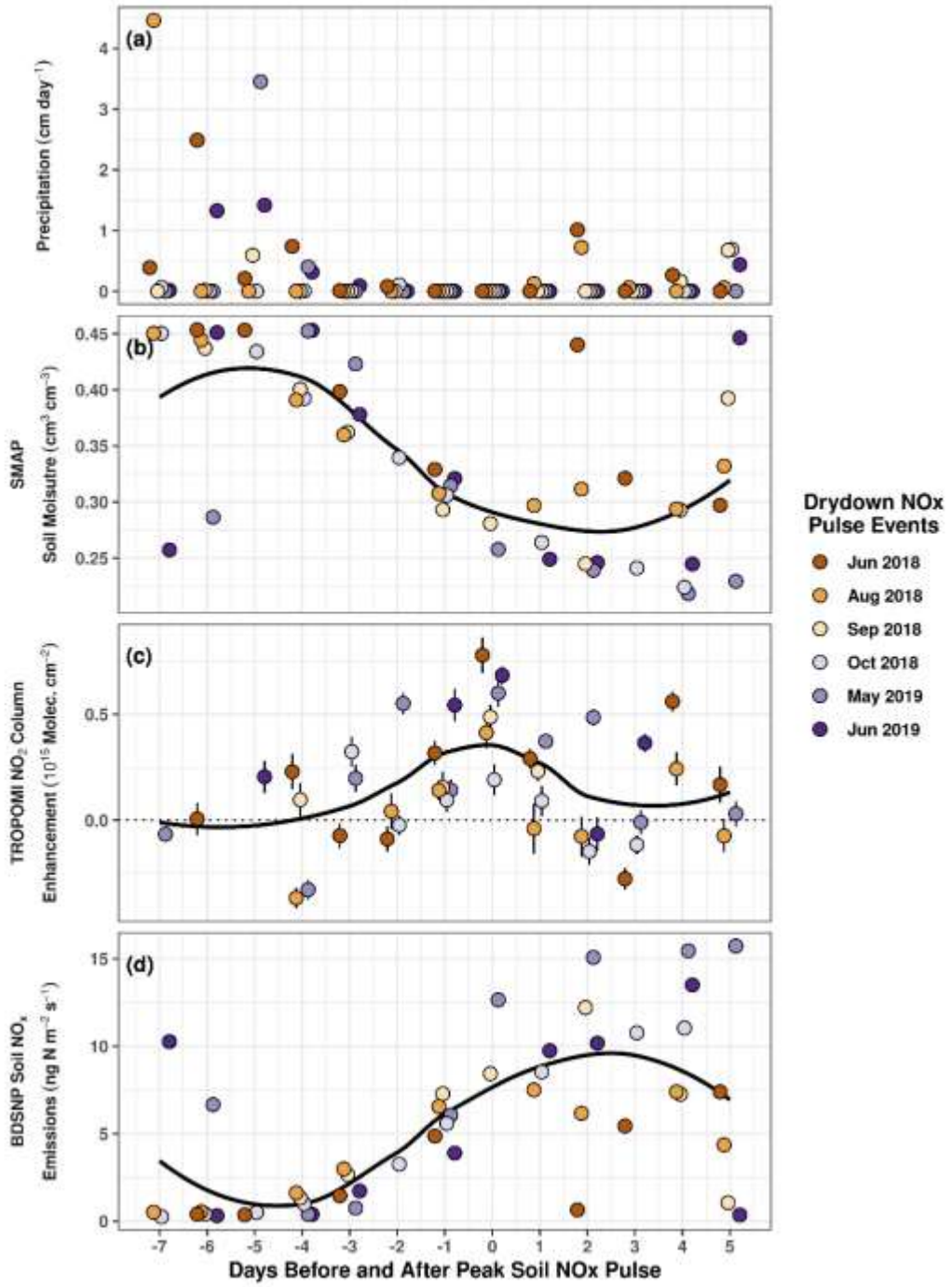

Figure 3: Time series for six drydown NO_x pulse events showing (a) NOAA CPC unified gauge-based precipitation, (b) observed SMAP VSM, (c) observed TROPOMI NO_2 column enhancements and (d) estimated BDSNP soil NO_x emissions. Data points for each day are slightly offset to aid visibility. Black curves represent smoothed local regression. Vertical standard error bars are included for SMAP and TROPOMI observations (panels b and c). Error bars in panel b are small and are covered by the markers. NO_2 column enhancements are defined as the VCD difference between the cropland box and the upwind box (Fig. 1a). Day 0 is defined as the day on which the peak drydown NO_x pulse occurs following an observed decrease in SMAP observations to ~30% VSM.

The drydown NO_x pulsing we observe is distinct from NO_x pulsing as classically described in the literature. Soil NO_x pulsing is historically characterized by a substantial increase in soil NO emissions within hours after soil wetting following an antecedent dry period (Kim et al., 2012; Davidson, 1992). Here, we observe peak enhancements between 4 and 8 days after precipitation and in the absence of preceding dry periods (Fig. 3). A multi-day lag between soil wetting and peak soil NO_x pulse emissions is not unprecedented and is hypothesized in Hall et al. (1996). A lag of 2-7 days has been observed (McCalley and Sparks, 2008; Hickman et al., 2018), however both studies experience preceding dry conditions, a distinct difference from our findings.

We include BDSNP soil NO_x emissions estimates for the same period as the drydown pulse events to compare with the behavior in the observed NO_2 column enhancements (Fig. 3d). While BDSNP emissions increase following precipitation, emissions continue to increase even after the observed TROPOMI enhancements peak on day 0. This is a result of the modeled soil moisture dependency within the BDSNP which is designed to peak at 13% VSM (30% WFPS) in the cropland domain, causing BDSNP estimates to continue increasing as soils continue drying after day 0. This may explain the largest BDSNP emissions during September 2019 (Fig. 2), as that month was the only time during the study period during which VSM values approached, but did not reach, 13% for multiple days, causing the BDSNP to estimate greater emissions during that month. This implies that for some cropland soils, BDSNP may overestimate emissions at lower VSM, may underestimate emissions at higher VSM, and may not capture the pulsing during drydown periods identified in the satellite record.

5. Conclusions

We find that daily spatial TROPOMI NO_2 enhancements can be successfully used to quantify the contribution from cropland soil to the NO_2 column at the daily and the seasonal scale and can sufficiently resolve the spatial variability associated with soil NO_x emissions. The resolution of the TROPOMI NO_2 product provides a much higher density of observations compared to previous satellite products, allowing for soil NO_x emissions to be resolved in spatially-confined regions like the MS Delta. We show that daily TROPOMI NO_2 observations can be applied to a box model framework to quantify seasonal cropland soil NO_x emissions for 2018 and 2019. Monthly NO_2 enhancements peak in late spring and early summer, times at which agricultural activity increases and enhances cropland soil NO_x emissions. Peak monthly NO_2 enhancements shift from May in

2018 to June in 2019, a shift that coincides with a shift in the timing of crop planting between 2018 and 2019. This suggests that seasonal land management practices directly influence the contribution from cropland soils to the NO_2 column. Soil NO_x box model emissions estimates achieve an annual maximum ranging from 15 to 34 ng N m^{-2} s^{-1}, values that are within the range of other estimated soil NO_x emissions. Box model emissions estimates are higher than BDSNP estimates, with the box model exhibiting similar variability in annual soil NO_x emissions as predicted by the BDSNP model. The lower BDSNP estimates may arise as a consequence of not capturing emissions that peak at VSM values above 13% in the cropland domain.

Additionally, TROPOMI NO_2 enhancements can resolve drydown NO_x pulse emissions over cropland in conjunction with decreasing SMAP surface VSM observations in the days following precipitation. This highlights a unique application of two space-based instruments to observe daily environmental process controls that contribute to enhanced cropland NO_x emissions. The daily soil contribution to the NO_2 column during peak drydown NO_x pulsing ranges from 0.2 x 10^{15} molecules cm^{-2} (October 2018) to 0.8 x 10^{15} molecules cm^{-2} (June 2018), consistent with more abundant available soil nitrogen at the beginning of the growing season (May/June) and less abundant at the end of the growing season (October). During drydown NO_x pulsing, TROPOMI NO_2 enhancements peak in the week following precipitation once SMAP measurements decrease below a threshold of 30% VSM (65% WFPS). This implies that not all non-arid soils experience peak emissions at 30% WFPS as is currently implemented in the BDSNP, and that BDSNP emissions may be under- or overestimated in regions where different soil moisture responses exist.

Acknowledgements

This work was supported by NASA Grants 80NSSC20K0929, NNX16AM99G and NSF Grant No. 1650682. Data used in this paper downloaded from the Sentinel-5P Pre-Operations Data Hub (TROPOMI, https://s5phub.copernicus.eu/dhus/), National Snow and Ice Data Center (SMAP, https://nsidc.org/data/SPL3SMP_E/versions/3), and the ECMWF Climate Data Store (ERA winds, https://cds.climate.copernicus.eu/cdsapp#!/dataset/reanalysis-era5-single-levels?tab=overview).

References

Ashmore, M. R. (2005). Assessing the future global impacts of ozone on vegetation. *Plant, Cell and Environment*, 28(8), 949–964. https://doi.org/10.1111/j.1365-3040.2005.01341.x

Bertram, T. H., Heckel, A., Richter, A., Burrows, J. P., & Cohen, R. C. (2005). Satellite measurements of daily variations in soil NOx emissions. *Geophysical Research Letters*, 32(24), L24812. https://doi.org/10.1029/2005GL024640

Bouwman, A. F., Boumans, L. J. M., & Batjes, N. H. (2002). Emissions of N2O and NO from fertilized fields: Summary of available measurement data. *Global Biogeochemical Cycles*, 16(4), 6-1-6–13. https://doi.org/10.1029/2001gb001811

Chen, M., Shi, W., Xie, P., Silva, V. B. S., Kousky, V. E., Higgins, R. W., & Janowiak, J. E. (2008). Assessing objective techniques for gauge-based analyses of global daily precipitation. *Journal of Geophysical Research Atmospheres*, 113(4). https://doi.org/10.1029/2007JD009132

Colliander, A., Jackson, T. J., Bindlish, R., Chan, S., Das, N., Kim, S. B., et al. (2017). Validation of SMAP surface soil moisture products with core validation sites. *Remote Sensing of Environment*, 191, 215–231. https://doi.org/10.1016/j.rse.2017.01.021

Davidson, E.A. Pulses of Nitric Oxide and Nitrous Oxide Flux Following Wetting of Dry Soil: An Assessment of Probable Sources and Importance Relative to Annual Fluxes. *Ecological Bulletins*, no. 42, 1992, pp. 149–155.

de Gouw, J. A., Veefkind, J. P., Roosenbrand, E., Dix, B., Lin, J. C., Landgraf, J., & Levelt, P. F. (2020). Daily Satellite Observations of Methane from Oil and Gas Production Regions in the United States. *Scientific Reports*, *10*(1), 1–10. https://doi.org/10.1038/s41598-020-57678-4

Eberwein, J. R., Homyak, P. M., Carey, C. J., Aronson, E. L., & Jenerette, G. D. (2020). Large nitrogen oxide emission pulses from desert soils and associated microbiomes. *Biogeochemistry*, 1–12. https://doi.org/10.1007/s10533-020-00672-9

Entekhabi, D., Njoku, E. G., O'Neill, P. E., Kellogg, K. H., Crow, W. T., Edelstein, W. N., et al. (2010). The soil moisture active passive (SMAP) mission. *Proceedings of the IEEE*, *98*(5), 704–716. https://doi.org/10.1109/JPROC.2010.2043918

Guenther, A., Karl, T., Harley, P., Wiedinmyer, C., Palmer, P. I., & Geron, C. (2006). Atmospheric Chemistry and Physics. In *European Geosciences Union* (Vol. 6, Issue 11). www.atmos-chem-phys.net/6/3181/2006/

Hall, Sharon J., et al. (1996). NOx EMISSIONS FROM SOIL: Implications for Air Quality Modeling in Agricultural Regions. *Annual Review of Energy and the Environment*, vol. 21, no. 1, Annual Reviews Inc., pp. 311–46, doi:10.1146/annurev.energy.21.1.311.

Han, W., Yang, Z., Di, L., & Mueller, R. (2012). CropScape: A Web service based application for exploring and disseminating US conterminous geospatial cropland data products for decision support. *Computers and Electronics in Agriculture*, *84*, 111–123. https://doi.org/10.1016/j.compag.2012.03.005

Hersbach, H., Bell, B., Berrisford, P., Hirahara, S., Horányi, A., Muñoz-Sabater, J., et al. (2020). The ERA5 global reanalysis. *Quarterly Journal of the Royal Meteorological Society*. https://doi.org/10.1002/qj.3803

Hickman, J. E., Dammers, E., Galy-Lacaux, C., & van der Werf, G. R. (2018). Satellite evidence of substantial rain-induced soil emissions of ammonia across the Sahel. *Atmospheric Chemistry and Physics*, 18(22), 16713–16727. https://doi.org/10.5194/acp-18-16713-2018

Hudman, R. C., Moore, N. E., Mebust, A. K., Martin, R. v., Russell, A. R., Valin, L. C., & Cohen, R. C. (2012). Steps towards a mechanistic model of global soil nitric oxide emissions: implementation and space based-constraints. *Atmospheric Chemistry and Physics*, 12(16), 7779–7795. https://doi.org/10.5194/acp-12-7779-2012

Jaeglé, L., Martin, R. v., Chance, K., Steinberger, L., Kurosu, T. P., Jacob, D. J., et al. (2004). Satellite mapping of rain-induced nitric oxide emissions from soils. *Journal of Geophysical Research D: Atmospheres*, 109(21). https://doi.org/10.1029/2004JD004787

Jenkin, M. E., & Clemitshaw, K. C. (2000). Ozone and other secondary photochemical pollutants: Chemical processes governing their formation in the planetary boundary layer.

Atmospheric Environment (Vol. 34, Issue 16, pp. 2499–2527). Elsevier Science Ltd. https://doi.org/10.1016/S1352-2310(99)00478-1

Jiang, Z., McDonald, B. C., Worden, H., Worden, J. R., Miyazaki, K., Qu, Z., et al. (2018). Unexpected slowdown of US pollutant emission reduction in the past decade. *Proceedings of the National Academy of Sciences of the United States of America*, 115(20), 5099–5104. https://doi.org/10.1073/pnas.1801191115

Kampa, M., & Castanas, E. (2008). Human health effects of air pollution. *Environmental Pollution*, 151(2), pp. 362–367). Elsevier. https://doi.org/10.1016/j.envpol.2007.06.012

Kim, D.-G., Vargas, R., Bond-Lamberty, B., & Turetsky, M. R. (2012). Effects of soil rewetting and thawing on soil gas fluxes: a review of current literature and suggestions for future research. *Biogeosciences*, 9(7), 2459–2483. https://doi.org/10.5194/bg-9-2459-2012

Kort, E. A., Frankenberg, C., Miller, C. E., & Oda, T. (2012). Space-based observations of megacity carbon dioxide. *Geophysical Research Letters*, *39*(17). https://doi.org/10.1029/2012GL052738

Laughner, J. L., & Cohen, R. C. (2019). Direct observation of changing NOx lifetime in North American cities. *Science*, 366(6466), 723–727. https://doi.org/10.1126/science.aax6832

Levine, J. S., Winstead, E. L., Parsons, D. A. B., Scholes, M. C., Scholes, R. J., Cofer, W. R., et al. (1996). Biogenic soil emissions of nitric oxide (NO) and nitrous oxide (N2O) from savannas in South Africa: The impact of wetting and burning. *Journal of Geophysical Research: Atmospheres*, 101(D19), 23689–23697. https://doi.org/10.1029/96JD01661@10.1002/(ISSN)2169-8996.TRACEA1

Linn, D. M., & Doran, J. W. (1984). Effect of Water-Filled Pore Space on Carbon Dioxide and Nitrous Oxide Production in Tilled and Nontilled Soils. *Soil Science Society of America Journal*, *48*(6), 1267–1272. https://doi.org/10.2136/sssaj1984.03615995004800060013x

Ludwig, J., Meixner, F. X., Vogel, B., & Forstner, J. (2001). Soil-air exchange of nitric oxide: An overview of processes, environmental factors, and modeling studies. *Biogeochemistry*, 52(3), 225–257. https://doi.org/10.1023/A:1006424330555

Martin, R. v., Jacob, D. J., Chance, K., Kurosu, T. P., Palmer, P. I., & Evans, M. J. (2003). Global inventory of nitrogen oxide emissions constrained by space-based observations of NO2 columns. *Journal of Geophysical Research D: Atmospheres*, 108(17). https://doi.org/10.1029/2003jd003453

McCalley, C. K., & Sparks, J. P. (2008). Controls over nitric oxide and ammonia emissions from Mojave Desert soils. *Oecologia*, 156(4), 871–881. https://doi.org/10.1007/s00442-008-1031-0

Oikawa, P. Y., Ge, C., Wang, J., Eberwein, J. R., Liang, L. L., Allsman, L. A., Grantz, D. A., & Jenerette, G. D. (2015). Unusually high soil nitrogen oxide emissions influence air quality in a high-temperature agricultural region. *Nature Communications*, 6(1), 1–10. https://doi.org/10.1038/ncomms9753

Pilegaard, K. (2013). Processes regulating nitric oxide emissions from soils. Philosophical *Transactions of the Royal Society B: Biological Sciences*, 368(1621), 20130126. https://doi.org/10.1098/rstb.2013.0126

Rasool, Q. Z., Zhang, R., Lash, B., Cohan, D. S., Cooter, E. J., Bash, J. O., et al. (2016). Enhanced representation of soil NO emissions in the Community Multiscale Air Quality (CMAQ) model version 5.0.2. *Geoscientific Model Development*, *9*(9), 3177–3197. https://doi.org/10.5194/gmd-9-3177-2016

Roelle, P. A., Aneja, V. P., Gay, B., Geron, C., & Pierce, T. (2001). Biogenic nitric oxide emissions from cropland soils. *Atmospheric Environment*, 35(1), 115–124. https://doi.org/10.1016/S1352-2310(00)00279-X

Schindlbacher, A., Zechmeister-Boltenstern, S., & Butterbach-Bahl, K. (2004). Effects of soil moisture and temperature on NO, NO2, and N 2O emissions from European forest soils. *Journal of Geophysical Research D: Atmospheres*, *109*(17). https://doi.org/10.1029/2004JD004590

Shah, V., Jacob, D. J., Li, K., Silvern, R. F., Zhai, S., Liu, M., Lin, J., & Zhang, Q. (2020). Effect of changing NOx lifetime on the seasonality and long-term trends of satellite-observed

tropospheric NO2 columns over China. *Atmospheric Chemistry and Physics*, 20(3), 1483–1495. https://doi.org/10.5194/acp-20-1483-2020

Shellito, P. J., Small, E. E., Colliander, A., Bindlish, R., Cosh, M. H., Berg, A. A., et al.. (2016). SMAP soil moisture drying more rapid than observed in situ following rainfall events. *Geophysical Research Letters*, 43(15), 8068–8075. https://doi.org/10.1002/2016GL069946

Silvern, R. F., Jacob, D. J., Mickley, L. J., Sulprizio, M. P., Travis, K. R., Marais, E. A., et al. (2019). Using satellite observations of tropospheric NO_2 columns to infer long-term trends in US NOx emissions: the importance of accounting for the free tropospheric NO_2 background. *Atmos. Chem. Phys*, 19, 8863–8878. https://doi.org/10.5194/acp-19-8863-2019

Strum, M., Eyth, A., & Vukovich, J. (2017). Preparation of Emissions Inventories for the Version 7, 2014 Emissions Modeling Platform for NATA. U.S. *Environmental Protection Agency*. Available online at. https://gaftp.epa.gov/Air_Quality_Data/emismod/2014/v1/reports/2014v7.0_2014_EmisMod_TSDv1.pdf

U.S. Department of Agriculture (USDA), National Agricultural Statistics Service. Crop Progress. Accessed November 3, 2019. https://usda.library.cornell.edu/concern/publications/8336h188j?locale=en

U.S. Environmental Protection Agency (EPA). Inventory of U.S. Greenhouse Gas Emissions and Sinks: 1990 - 2016. EPA 430- R-18-003. https://www.epa.gov/sites/production/files/2018-01/documents/2018_complete_report.pdf.

van Geffen, J.H.G.M., et al. "TROPOMI ATBD of the Total and Tropospheric NO2 Data Products." KNMI, 2019. Available on-line at http://www.tropomi.eu/sites/default/files/files/publicS5P-KNMI-L2-0005-RP-ATBD_NO2_data_products-20190206_v140.pdf

Veefkind, J. P., Aben, I., McMullan, K., Förster, H., de Vries, J., Otter, G., et al. (2012). TROPOMI on the ESA Sentinel-5 Precursor: A GMES mission for global observations of the atmospheric composition for climate, air quality and ozone layer applications. *Remote Sensing of Environment*, *120*, 70–83. https://doi.org/10.1016/j.rse.2011.09.027

Vinken, G. C. M., Boersma, K. F., Maasakkers, J. D., Adon, M., & Martin, R. v. (2014). Worldwide biogenic soil NOx emissions inferred from OMI NO2 observations. *Atmos. Chem. Phys*, 14, 10363–10381. https://doi.org/10.5194/acp-14-10363-2014

Yan, X., Ohara, T., & Akimoto, H. (2005). Statistical modeling of global soil NOX emissions. *Global Biogeochemical Cycles*, *19*(3), 1–15. https://doi.org/10.1029/2004GB002276

Yang, R., Hayashi, K., Zhu, B., Li, F., & Yan, X. (2010). Atmospheric NH3 and NO2 concentration and nitrogen deposition in an agricultural catchment of Eastern China. *Science of The Total Environment*, *408*(20), 4624–4632. https://doi.org/10.1016/J.SCITOTENV.2010.06.006

Zörner, J., Penning De Vries, M., Beirle, S., Sihler, H., Veres, P. R., Williams, J., & Wagner, T. (2016). Multi-satellite sensor study on precipitation-induced emission pulses of NOx from soils in semi-arid ecosystems. *Atmospheric Chemistry and Physics*, 16(14), 9457–9487. https://doi.org/10.5194/acp-16-9457-2016